Progress in Natural Science: Materials International 27 (2017) 498–502

HOSTED BY

Contents lists available at ScienceDirect

Progress in Natural Science: Materials International

journal homepage: www.elsevier.com/locate/pnsmi

Original Research

Temperature-dependent optical resonance in a thin-walled tubular oxide microcavity

Yangfu Fang[a], Xianyun Lin[a], Shiwei Tang[b], Borui Xu[a], Jiao Wang[a,c], Yongfeng Mei[a,*]

[a] Department of Materials Science, Fudan University, Shanghai 200433, China
[b] Department of Physics, Faculty of Science, Ningbo University, Ningbo, Zhejiang 315211, China
[c] School of Information Science & Engineering, Fudan University, Shanghai 200433, China

ARTICLE INFO

Keywords:
Microcavities
Rolled-up
Whispering gallery mode (WGM)
Temperature-response
Mie scattering method

ABSTRACT

This work proposes a temperature-response capability of optical resonance in tubular optical oxide microcavities. The thin wall thickness with a subwavelength scale enables these microcavities to interact with the environment effectively. By optimization of the geometries and materials, the tubular microcavities can be tuned into temperature-inert in vacuum, and the experiments support this design. The experiments prove the idea of utilizing them as temperature-inert microcavities. Contrary wavelength shifts from previous studies were observed, which can be explained with the theoretical model. Furthermore, the theoretical results of the present work suggest that novel rolled-up microtubes could act as an exceptional optical microcavity for the application in temperature response.

1. Introduction

With their distinct feature of high quality factor (Q factor) and small mode volume, the optical whispering-gallery modes (WGMs) in dielectric microcavities have been extensively used in the applications such as photonics filters [1–4], cavity quantum electrodynamics [5,6], bio-molecule sensors [7], low threshold lasers [8,9] and nonlinear optics [10]. Small changes in the geometry or refractive index of the dielectric microcavity system may cause a significant resonance wavelength shift for a given WGM [9], which could be induced by thermal fluctuations from the variation of ambient temperature or the absorption of laser energy during the laser scanning or pumping, leading to thermal instability. The temperature-related shifting of WGMs in microresonators can be a help or a hindrance depending on the application [11]. For example, the ultrasensitive mode shifting in the WGM resonance to the surrounding temperature can be utilized to design high-sensitivity thermal sensor [12] or allow thermal tuning of the lasing mode [13], the thermal nonlinearity induced optical bistability can make a useful optical switch [14]. On the other hand, in label-free biological-chemical sensing the thermally induced drifting can be a source of thermal noise that needs to be reduced [15]. Moreover, strong thermo-optic effect would mask the Kerr-driven variations in the refractive index so that the observation of the Kerr effect can be restrained [16–18]. Therefore, finding a way to reduce or even cancel this thermal effect of WGMs is highly desired. A practical approach is to introduce materials with a negative thermal refraction coefficient in the vicinity of the WGM microcavities to compensate the resonance wavelength shift due to their positive thermal refraction coefficient [14,19], which, in turn, could influence the intrinsic resonance behaviors of the WGMs.

Different behaviors of resonances are shown as the temperature changes for different materials, geometry or circumstance of our self-rolled up microtubes correspondingly. We tested the resonance property of these tubular optical microcavities under various temperatures and found out the contrary mode shift directions between our work and previous work [20,21]. These structures are based on a new class of microcavities with WGMs in a tubular or hollow cylindrical geometry [1,22–24], which have been comprehensively studied in both theoretical and experimental aspects for potential applications including optofluidic devices, integrated optics and sensors in lab-on-a-chip applications [9,25,26]. Moreover, the tubular microcavities rolled up from pre-strained films have been demonstrated with superior sensing performance owing their sub-wavelength wall thickness [29–31]. For example, we take the tubular microcavities fabricated from Y_2O_3/ZrO_2 bilayer nanomembrane based on the self-rolled process with wet chemical method. To improve the Q factor, the oxide tubular microcavity arrays are uniformly coated with 50 nm alumina oxide by atomic layer deposition (ALD), as shown in Fig. 1(a). The microtube consists

Peer review under responsibility of Chinese Materials Research Society.
* Corresponding author.
E-mail address: yfm@fudan.edu.cn (Y. Mei).

http://dx.doi.org/10.1016/j.pnsc.2017.03.011
Received 18 January 2017; Accepted 22 March 2017
Available online 03 August 2017

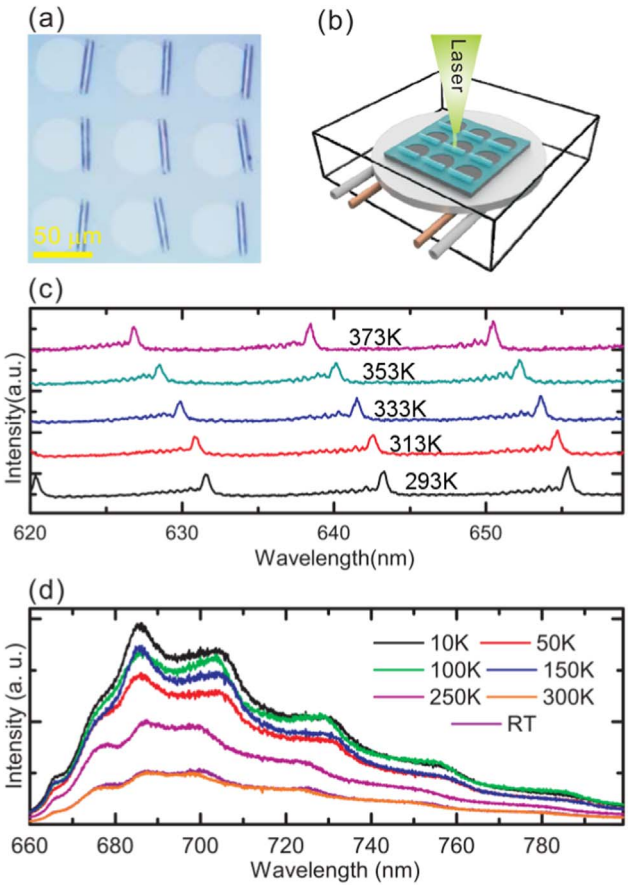

Fig. 1. (a) Optical microscopy image of oxide tubular microcavity arrays after the ALD coating. (b) Schematic diagram of μ-PL measurement under different temperature and nitrogen atmosphere. (c) The μ-PL spectra of a rolled-up microcavity under different temperature of the above Y_2O_3/ZrO_2 tube in air. (d) The μ-PL spectra of SiO/SiO_2 tubular optical microcavities in nitrogen gas.

of Y_2O_3/ZrO_2 layers wrapped by ALD for 50 nm and thicknesses of Y_2O_3/ZrO_2 are 8/24 nm, respectively. The temperature controlling device is shown in Fig. 1(b), where brown pipes with resistance wire inside heating the disk below the sample and white pipes bubble liquid nitrogen for cooling, thus we can arbitrarily control the temperature and the ambience. The optical properties of these microcavities were measured by a micro-photoluminescence (μ-PL) spectroscopy with an excitation line at 514 nm, under different measuring temperature. Fig. 1(c) indicated that the experimental thermal-induced resonance wavelength shows obvious blue shift when the temperature rises from room temperature (~ 293 K) to 373 K with the step of 20 K. In contrast, the resonance properties from the SiO/SiO_2 tubular optical microcavities fabricated by dry etching method, releasing pre-stressed SiO/SiO_2 bilayer nanomembranes from polymer sacrificial layers are also influenced by temperature, which is shown in Fig. 1(d). The resonance peaks in Fig. 1(c) presents obvious shifts compared with that in Fig. 1(d). This abnormal blue mode shift were observed in the previous experiments [20,21], which was considered resulting from dynamic desorption process of H_2O molecules when oxide terminated microtubes were heated. However, theoretical model suggests that only red shifts appear when there are only considered with geometry deformation and refractive index changing induced by thermal effect. Hence, it is demanded to establish a complete theory to describe such temperature-dependent resonance behaviors of our tubular microcavities.

In this work, the thermal stability and sensing capability of these rolled-up tubular microcavities are both theoretically and experimentally investigated. A theory is established to describe the resonance

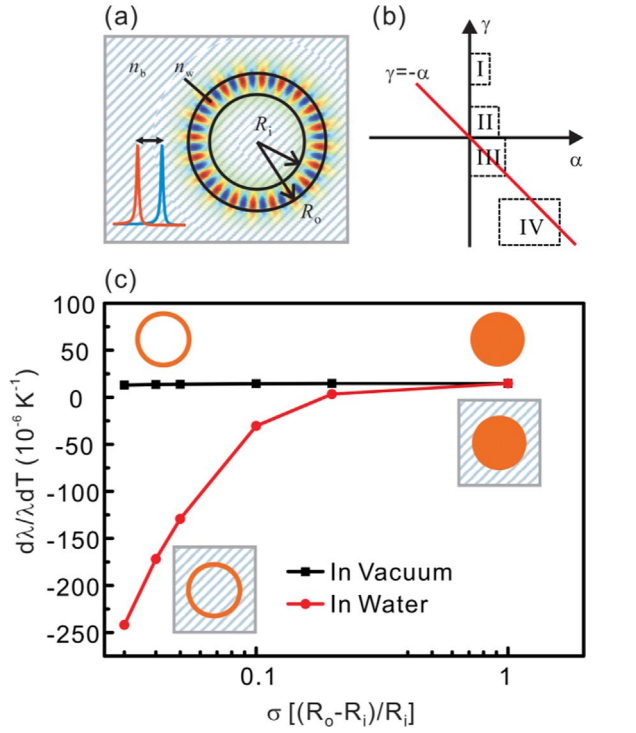

Fig. 2. (a) Sketch of a tubular microcavity. The inset in the left bottom corner exhibits wavelength shift when background refractive index n_b changes. (b) Materials map for thermal response in $\gamma-\alpha$ plane. I: semiconductors like Si, Ge; II: oxides like SiO_2, TiO_2; III: halides like CaF_2; IV: polymers like PS and PMMA. (c) Thermal response of microtubes made up with Al_2O_3 In vacuum and water. (For interpretation of the references to color in this figure, the reader is referred to the web version of this article).

wavelength shifts behaviors of the tubular microcavities. The theoretical result shows that, the tubular microcavities are potential to be fabricated temperature-inert in vacuum or temperature-sensitive in liquid media. To confirm this theory, a temperature-inert tubular microcavity is detected, which is different from the unstable tubular microcavities we mentioned above and is in good agreement with the theoretical results. These theoretically and experimentally results indicate that the WGMs in such rolled-up microcavities are expected to be less sensitive to the refractive index of the tube wall materials.

2. Theoretical model

As discussed above, the tubular microcavities with different structure, materials and circumstances have different behaviors of temperature-response. As a result, a complete theory system should be established to describe such behaviors of temperature-response of the tubular microcavities. In a realistic rolled-up microtube, the cross section of the tube is in a spiral shape, which could lead to the mode splitting and Q spoiling compared to an ideal tubular geometry [27,28]. For a simple one-layered microtube with an outer radius R_o and an inner radius R_i as shown in Fig. 2(a), we use $\sigma = (R_o - R_i)/R_i$ to identify its thickness. Combining the self-rolled-up technique with a following atomic layer deposition process of oxides, it can be well tuned with $0.01 < \sigma < 0.05$ in experiments [29,31,32]. It is worth to note that σ does not change with temperature (i.e. $d\sigma/dT = 0$) as the microtube is expanding uniformly. In addition, thermal expansion coefficient (CTE) of the microtube materials is represented by α, and we use the relative refractive index change (γ) to describe the thermo-optic effect (i.e. the refractive index of the tube wall material $n = n_0(1 + \gamma\Delta T)$, where n_0 is a constant coefficient and ΔT the temperature variation). Typical materials are selected in the γ-α plane of Fig. 2(b). For examples, Region I: some semiconductors like Si, Ge; Region II: oxides like SiO_2, TiO_2; Region III: halides like CaF_2; Region IV: polymers like PS and PMMA.

We don't need to consider Regions II and III because thermal properties α and γ are small enough. For Region I, although the thermo-optical coefficient γ is very high, minimum wavelength shift can be obtained by decreasing the tube wall thickness. Microtubes made by fused silica ($n_w = 1.4$, $\alpha = 0.55 \times 10^{-6}\ K^{-1}$, $\gamma = 12 \times 10^{-6}\ K^{-1}$) or other materials with small α could benefit from it. In the region IV, the microtubes made up with the materials between the straight line $\gamma = -\alpha$ and the γ axis could become temperature-inert.

When WGM resonance occurs in a tubular microcavity at wavelength λ, one has

$$n_{\mathrm{eff}} L = M\lambda, \tag{1}$$

where n_{eff} is the effective refractive index, $L = \pi(R_{\mathrm{i}} + R_{\mathrm{o}}) = \pi(2 - \sigma)R_{\mathrm{o}}$ is the circumference of the tube, and the integer M is the order index of the resonance. By differentiation, we can get thermal-induced resonance wavelength shift from Eq. (1):

$$\frac{\mathrm{d}\lambda}{\lambda \mathrm{d}T} = \frac{1}{L}\frac{\mathrm{d}L}{\mathrm{d}T} + \frac{1}{n_{\mathrm{eff}}}\frac{\mathrm{d}n_{\mathrm{eff}}}{\mathrm{d}T}. \tag{2}$$

Here we apply a waveguide approach to obtain the value of n_{eff}. If the tube wall is thin enough compared with its radius, the tube wall can be regarded as a flat film to supports waveguide modes with an effective refractive index n_{eff} satisfying the equation of [33]

$$\kappa\frac{2\pi}{\lambda}h = 2\tan^{-1}(a\frac{p}{\kappa}), \tag{3}$$

where $h = R_{\mathrm{o}} - R_{\mathrm{i}} = \sigma R_{\mathrm{o}}$, $\kappa^2 = n_{\mathrm{w}}^2 - n_{\mathrm{eff}}^2$, $p^2 = n_{\mathrm{eff}}^2 - n_{\mathrm{b}}^2$ and $a = 1$ for transverse magnetic modes (TM modes: the electric field is parallel to the tube axis) or $a = n_{\mathrm{w}}^2/n_{\mathrm{b}}^2$ for transverse electric modes (TE modes: the magnetic field is parallel to the tube axis). The refractive index of the tube wall is n_w and the circumstance refractive index is n_b. By substituting $L = \pi(2 - \sigma)R_{\mathrm{o}}$ into Eq. (3), we can easily find that n_{eff} is independent of R_{o}. That is reasonable in tubular microcavities because when σ is fixed the changing R_{o} is simply to scale the dimension of the microcavity. According to the scale-invariant nature of Maxwell's equations, the dimensions and time are scaled in equal proportion [34]. So the speed of light propagating in the microcavity keeps unchanged.

As discussed above one has $dn_{\mathrm{eff}}/dR = 0$ and $d\sigma/dT = 0$, dn_{eff}/dT can then be expressed in a simple partial differential form

$$\frac{\mathrm{d}n_{\mathrm{eff}}}{\mathrm{d}T} = \frac{\partial n_{\mathrm{eff}}}{\partial n_{\mathrm{w}}}\frac{\mathrm{d}n_{\mathrm{w}}}{\mathrm{d}T} + \frac{\partial n_{\mathrm{eff}}}{\partial n_{\mathrm{b}}}\frac{\mathrm{d}n_{\mathrm{b}}}{\mathrm{d}T}, \tag{4}$$

As a result, the thermal-induced resonance wavelength shift can be described as the following equation:

$$\frac{\mathrm{d}\lambda}{\lambda \mathrm{d}T} = \alpha + G_{\mathrm{w}}\gamma_{\mathrm{w}} + G_{\mathrm{b}}\gamma_{\mathrm{b}}, \tag{5}$$

where $G_w = \partial n_{eff}/\partial n_w \cdot n_w/n_{eff}$ and $G_b = \partial n_{eff}/\partial n_b \cdot n_b/n_{eff}$. Intuitively, G_w and G_b in Eq. (5) can be understood as energy fraction of WGM fields in the tube wall and circumstance, respectively. The light energy fractions stand for the amount of light energy in different regions, which can be calculated by integrating the light energy over the corresponding regions in simulation [19,33].

3. Discussion

3.1. Design

Based on Eq. (5) we can derive many interesting properties of tubular microcavities. One has $n_{\mathrm{eff}} \approx n_w$ if the resonance energy is highly confined within the microcavity wall with a high Q factor, which is the case of $G_w \approx 1$ and $G_b \approx 0$. On the contrary, if the resonance mode is too weak to confine light within the microcavity wall, $n_{\mathrm{eff}} \approx n_b$ is excepted, corresponding to the case of $G_w \approx 0$ and $G_b \approx 1$. Therefore, it is reasonable to point out that $0 < G_w < 1$ and $0 < G_b < 1$ for a realistic tubular microcavity because of the presence of the evanescent field near the interface. And, one can tune the contribution of G_w and G_b in Eq. (5) by varying the wall thickness as shown in Fig. 2(c) where the thermal sensitivity ($d\lambda/dT$) of a tubular microcavity in vacuum (black line and squares) and water (red line and circles) are calculated. In vacuum, the tubular microcavity with a thinner wall thickness has a small G_w, leading to a temperature-inert response. On the contrary, this microcavity presents a great temperature sensitivity in water, because G_b now contributes more than G_w. For example, the thermal sensitivity of a microcavity with $\sigma = 0.03$ in water is 18.5 times higher than that in vacuum.

It is important to understand the thermal response for the condition of a tubular microcavity in vacuum. In this case, $n_b = 1$, $\gamma_b = 0$ and n_{eff} can be solved based on Eq. (3) for both TE and TM modes with a mode index of $M = 40$ on different thickness (σ). Then G_w is obtained directly from its definition $G_{\mathrm{w}} = \partial n_{\mathrm{eff}}/\partial n_{\mathrm{w}} \cdot n_{\mathrm{w}}/n_{\mathrm{eff}}$. It is shown that G_w can be tuned between 0 and 1 by changing the tube geometry or material's refractive index. From previous works, we have noticed that the thermal-induced wavelength shifts of other WGM microcavities, for example microspheres and microdisks, are governed by similar equations like Eq. (5) [35,36]. For these high-Q microcavities, n_{eff} is usually replaced by the cavity's refractive index n_w in this equation so that G_w is always unity and G_b equals zero. For the microtubes in this study with subwavelength wall thickness, the evanescent field can easily penetrate into the background medium. The leakage of light in the form of the evanescent field is the main reason why the Q factors of the microtubes are much lower than that of microspheres or microtoroids [24]. Nevertheless, owing to the ability of sharing light energy with the environment, the microtubes with a subwavelength wall thickness offer possibilities like circumstance detection or self-thermal compensation, as will be discussed in detail in following section.

To obtain a temperature-inert microcavity (i.e. $d\lambda/dT = 0$ in Eq. (5)), one has

$$\alpha + G_{\mathrm{w}}\gamma_{\mathrm{w}} = 0 \tag{6}$$

Typical materials [37] are selected in the γ–α plane of Fig. 2(b). For example, Region I: semiconductors like Si, Ge; Region II: oxides like SiO_2, TiO_2; Region III: halides like CaF_2; Region IV: polymers like PS and PMMA. Regions II and III are not needed to be considered because α and γ in these regions are small enough. For Region I, although the thermo-optical coefficient γ is very high, the wavelength shift can be minimized by decreasing the tube wall thickness (when G_w approaching 0). Microtubes made by fused silica ($n_w = 1.4$, $\alpha = 12 \times 10^{-6}\ K^{-1}$ and $\gamma = 0.55 \times 10^{-6}\ K^{-1}$) or other materials with a small α could be benefit from it. In Region IV, the microtubes made up with the materials between the straight line $\gamma = -\alpha$ and the γ axis could become temperature-inert. For example, a microtube made by PS ($n_w = 1.5$, $\alpha = 70 \times 10^{-6}\ K^{-1}$ and $\gamma = -95 \times 10^{-6}\ K^{-1}$) is temperature-inert if it is well-designed to have a $G_w = 0.74$. With materials satisfying $-\alpha/\gamma < 0$ (in Region I and II), obtaining a self-compensated microcavity is impossible.

As discussed above, G_w dominates Eq. (5) to obtain a temperature-inert microcavity. As shown in Fig. 3, a microtube with a large σ have $G_w \approx 1$, while microtubes with a thin wall thickness enable G_w varying from 1 to 0 dramatically, especially for those with a lower refractive index. As has been discussed above, this is caused by the interaction of the optical resonance and the circumstance. For the tubular microcavities, a smaller σ means a thinner tube wall so that less light energy is confined in the microcavity and G_w is smaller. Similarly, a smaller n_w weaken the light confinement and results in the decrement of G_w. From Fig. 3, we can clearly see that a relative low refractive index ($n_w < 2$) and ultrathin tube wall thickness ($\sigma < 0.1$) offer one of the most effective ways to tune G_w down to a small value. Rolled-up tubular microcavities with a subwavelength wall thickness are supposed to be suitable for a wide range of tuning G_w. In Ref. [31], it is reported that there was almost no shift observed in resonance peaks of rolled-up SiO/Si

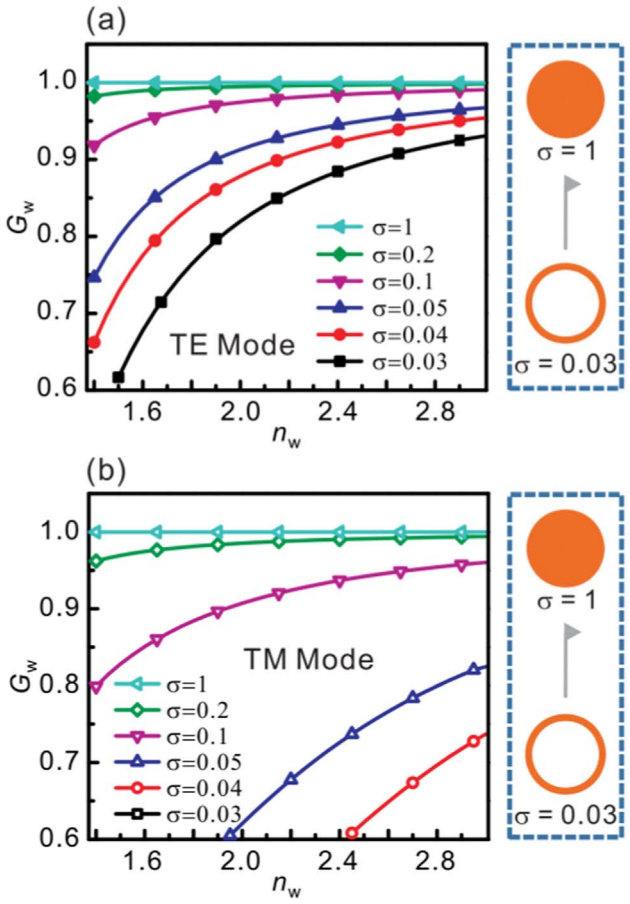

Fig. 3. G_w of microtubes as a function of the refractive index of wall materials for (a) TE modes and (b) TM modes with a mode index of M = 40.

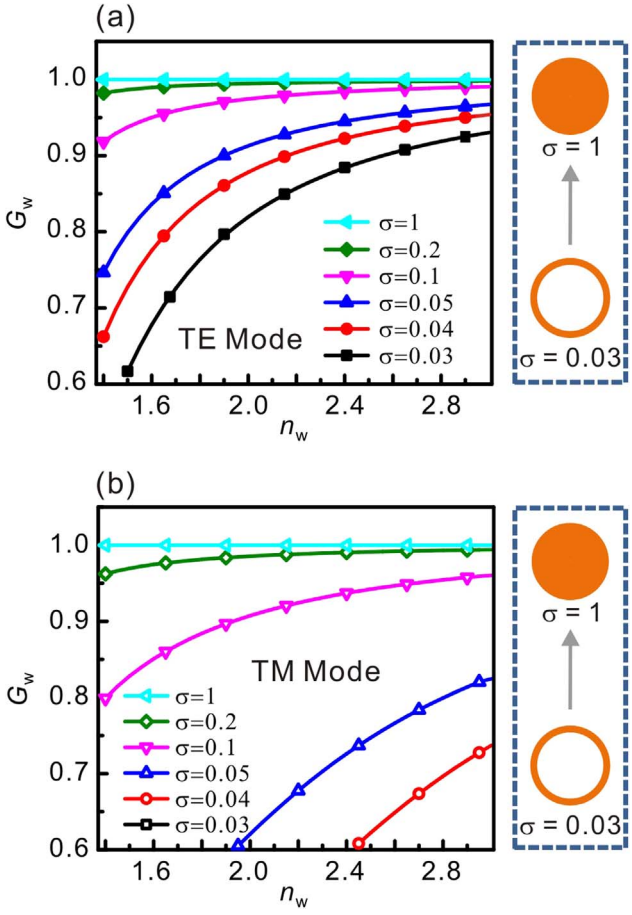

Fig. 4. The μ-PL spectra of a rolled-up microcavity under different temperature. A subtle redshift of resonance wavelengths can be seen.

microtubes when the measurement temperature was cooling from room temperature to 11 K. We also found that TE modes lead to smaller G_w values than TM modes, which mainly results from their different abilities to confine light in the tube wall [38,39]. Meanwhile, TE modes have a lower Q factor than TM modes, and are usually difficult to be observed in experiments.

3.2. Experimental characterization compared with modeling

To shed light on the thermal stability and sensing capability of these rolled-up tubular microcavities, the interferences such as the water vapor or adsorbate form air should be removed. As a result, we passed over the nitrogen into the device, which is shown in Fig. 1(b). To confirm the thermal stability of the tubular microcavities, the experiments were carried out. In this work, the tubular microcavities were fabricated from Y_2O_3/ZrO_2 bilayer nanomembrane based on the wet chemical self-rolled process. A photoresist layer was coated on a Si wafer and defined into circles with a diameter of 80 μm by photolithography, served as a sacrificial layer in the following rolling process. After the deposition of strained Y_2O_3/ZrO_2 bilayers with glancing angle on top of the photoresist (which can guarantee the tubes attached on substrates), the photoresist layer was selectively removed with acetone and the strained Y_2O_3/ZrO_2 bilayer was released and self-assemble into a tubular microcavity. The thickness of the Y_2O_3 layer the ZrO_2 layer was 8 nm and 24 nm, respectively. The rolled-up oxide tubular microcavities were then dried in the critical point dryer by using liquid CO_2 as an inter-medium to avoid the collapse of the tubular structures and then coated by ALD for 50 nm with a better mechanical strength. The rolled-up tubular microcavities had an approximate outer radius of 9 μm. And optical properties of these microcavities were measured by a μ-PL spectroscopy with an excitation line at 514 nm.

After passing over the nitrogen into the device, from the μ-PL spectroscopy shown in Fig. 4 we can find that the resonance wavelength almost has nothing to do with the temperature, which means that the tubular microcavities become temperature-inert. Such condition is quite different from the temperature sensitive phenomena we mentioned above [20,21].

For the experimental results, the diameter of microtubes is approximately 9 μm and the thickness 190 nm (including Al_2O_3 post-coating layer), thus $\sigma = 0.04$. As the refractive index of Y_2O_3/ZrO_2 is known (about 1.9 [37]), G_w is 0.85. Then the thermal-induced wavelength shift of the microtubes in vacuum can be inferred from the thermal property of Y_2O_3/ZrO_2 and Eq. (5) should be $d\lambda/\lambda dT = \alpha + G_w\gamma = 12.0 \times 10^{-6}\ K^{-1}$, where $\alpha = 8.8 \times 10^{-6}\ K^{-1}$ and $\gamma = 3.75 \times 10^{-6}\ K^{-1}$ are taken [40]. At resonance wavelength around 624 nm, the theoretical sensitivity of the microtubes will be around 7.48 pm/K. It is smaller than that of the silicon based WGM microcavities [41], although the thermal stability of silicon ($\alpha = 0.55 \times 10^{-6}\ K^{-1}$, $\gamma = 9.14 \times 10^{-6}\ K^{-1}$) is better than that of Y_2O_3/ZrO_2. As is shown in Fig. 5, the experimental thermal-induced resonance wavelength shifts fit well with our theoretical ones. An average wavelength shift of 7.1 pm/K was observed at around 624 nm, which is comparable to the theoretical 7.48 pm/K. To further verify our theory, a more accurate Mie scattering method was applied to calculate the resonance wavelength under different temperature (see the straight lines in Fig. 5). The theoretical results on resonance wavelength shifts fit well with the experimental results. The slight offset is mainly attributed to the spiral geometry, deviated geometry and/or material parameters of rolled up microtubes, which could be improved with further optimization.

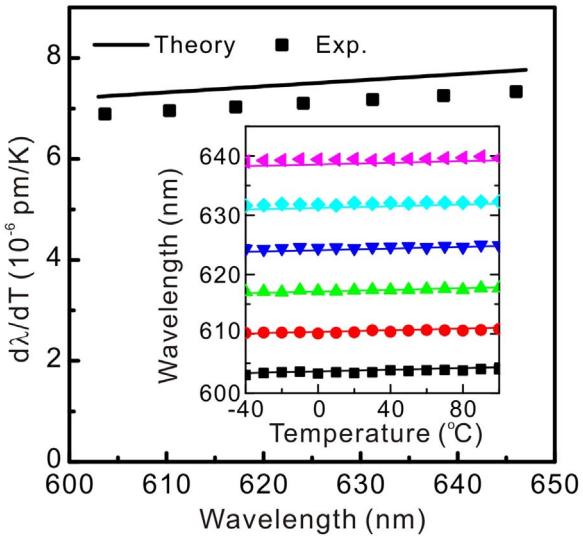

Fig. 5. Theoretical thermal-induced resonance wavelength shifts (in solid line) and experimental data (in squares). In the inset, peak positions for each resonances are plotted in shapes (squares, circles, etc.), and fitted resonance wavelengths (Mie scattering method) in straight lines.

4. Conclusions

A complete theory system based on planar waveguide model and Mie scattering method to describe such behaviors of temperature-response of the tubular microcavities have been established in the present study. And the resonance properties of the tubular microcavities with a subwavelength wall thickness fabricated by rolling-up process have also been experimentally investigated, which is in good agreement with the theory. This work could be useful for the design of unique thermal-stable optical micro-devices and micro-sensors.

Acknowledgements

This work was supported by the National Natural Science Foundation of China (Nos. 51322201, 51302039, 11604167), the Changjiang Young Scholars Programme of China and Science and Technology Commission of Shanghai Municipality (No. 14JC1400200).

References

[1] A. Bernardi, S. Kiravittaya, A. Rastelli, R. Songmuang, D.J. Thurmer, M. Benyoucef, O.G. Schmidt, Appl. Phys. Lett. 93 (2008) 94106.
[2] F. Monifi, K. Özdemir, L. Yang, Appl. Phys. Lett. 103 (2013) 181103.
[3] F. Monifi, J. Friedlein, K. Özdemir, L. Yang, J. Lightwave Technol. 30 (2012) 3306–3315.
[4] A.M. Prabhu, V. Van, Opt. Express 15 (2007) 9645–9658.
[5] T. Aoki, B. Dayan, E. Wilcut, W.P. Bowen, A.S. Parkins, T.J. Kippenberg, K.J. Vahala, H.J. Kimble, Nature 443 (2006) 671–674.
[6] Y. Park, A.K. Cook, H. Wang, Nano Lett. 6 (2006) 2075–2079.
[7] I.M. White, N.M. Hanumegowda, X. Fan, Opt. Lett. 30 (2005) 3189–3191.
[8] L. He, K. Özdemir, L. Yang, Laser Photonics Rev. 7 (2013) 60–82.
[9] D.K. Armani, T.J. Kippenberg, S.M. Spillane, K.J. Vahala, Nature 421 (2003) 925–928.
[10] V.S. Ilchenko, A.A. Savchenkov, A.B. Matsko, L. Maleki, Phys. Rev. Lett. 92 (2004) 43903.
[11] J.M. Warda, N. Dhasmana, S.N. Chormaic, Eur. Phys. J. Spec. Top. 223 (2014) 1917–1935.
[12] B. Li, Q. Wang, Y. Xiao, X. Jiang, Y. Li, L. Xiao, Q. Gong, Appl. Phys. Lett. 96 (2010) 251109.
[13] J.M. Ward, Y. Yang, S.N. Chormaic, Sci. Rep. 6 (2016) 25152.
[14] I. Grudinin, H. Lee, T. Chen, K. Vahala, Opt. Express 19 (2011) 7365–7372.
[15] J.D. Suter, I.M. White, H. Zhu, X. Fan, Appl. Opt. 46 (2007) 389–396.
[16] V.S. Ilchenko, M.L. Gorodetskii, Laser Phys. 2 (1992) 1004–1009.
[17] F. Treussart, V.S. Ilchenko, J. Roch, J. Hare, V. Lefevre-Seguin, J. Raimond, S. Haroche, Eur. Phys. J. D 1 (1998) 235–238.
[18] V.B. Braginsky, M.L. Gorodetsky, V.S. Ilchenko, Phys. Lett. A 137 (1989) 393–397.
[19] L. He, Y. Xiao, C. Dong, J. Zhu, V. Gaddam, L. Yang, Appl. Phys. Lett. 93 (2008) 201102.
[20] J. Zhong, J. Wang, G. Huang, G. Yuan, Y. Mei, Nanoscale Res. Lett. 8 (2013) 531.
[21] L. Ma, S. Li, V.A.B. Quiñones, L. Yang, W. Xi, M. Jorgensen, S. Baunack, Y. Mei, S. Kiravittaya, O.G. Schmidt, Adv. Mater. 25 (2013) 2357–2361.
[22] X. Fan, I.M. White, Nat. Photonics 5 (2011) 591–597.
[23] Y. Sun, X. Fan, Opt. Express 16 (2008) 10254–10268.
[24] J. Wang, T. Zhan, G. Huang, P.K. Chu, Y. Mei, Laser Photonics Rev. 8 (2014) 521–547.
[25] A. Ksendzov, Y. Lin, Opt. Lett. 30 (2005) 3344–3346.
[26] M. Han, A. Wang, Opt. Lett. 32 (2007) 1800–1802.
[27] Y. Fang, S. Li, Y. Mei, Phys. Rev. A 94 (2016) 033804.
[28] S. Li, L. Ma, S. Böttner, Y. Mei, M.R. Jorgensen, S. Kiravittaya, O.G. Schmidt, Phys. Rev. A, 88, 033833.
[29] G. Huang, V.A.B. Quinones, F. Ding, S. Kiravittaya, Y. Mei, O.G. Schmidt, ACS Nano 4 (2010) 3123–3130.
[30] F. Zhao, T. Zhan, G. Huang, Y. Mei, X. Hu, Lab Chip 12 (2012) 3798–3802.
[31] J. Zhang, J. Zhong, Y.F. Fang, J. Wang, G.S. Huang, X.G. Cui, Y.F. Mei, Nanoscale 6 (2014) 13646–13650.
[32] J. Wang, T. Zhan, G. Huang, X. Cui, X. Hu, Y. Mei, Opt. Express 20 (2012) 18555–18567.
[33] T. Zhan, C. Xu, F. Zhao, Z. Xiong, X. Hu, G. Huang, Y. Mei, J. Zi, Appl. Phys. Lett. 99 (2011) 211104.
[34] J.D. Joannopoulos, S.G. Johnson, J.N. Winn, R.D. Meade, Photonic Crystals: Molding the Flow of Light, Princeton University Press, Princeton, New Jersey, USA, 2011.
[35] J. Zhu, S.K. Oezdemir, L. He, L. Yang, Appl. Phys. Lett. 99 (2011) 171101.
[36] C. Dong, L. He, Y. Xiao, V.R. Gaddam, S.K. Ozdemir, Z. Han, G. Guo, L. Yang, Appl. Phys. Lett. 94 (2009) 231119.
[37] E.D. Palik, Handbook of Optical Constants of Solids, Academic Press, San Diego, US, 1998.
[38] T. Kipp, H. Welsch, C. Strelow, C. Heyn, D. Heitmann, Phys. Rev. Lett. 96 (2006) 77403.
[39] G.S. Huang, S. Kiravittaya, V.Q. Ones, F. Ding, M. Benyoucef, Appl. Phys. Lett. 94 (2009) 141908.
[40] G. Ghosh, Handbook of Thermo-Optic Coefficients of Optical Materials with Applications, Academic, New York, 1998.
[41] L.L. Martín, C. Pérezrodríguez, P. Harogonzález, I.R. Martín, Opt. Express 19 (2011) 25792–25798.